ELSEVIER

Thermochimica Acta 269/270 (1995) 523–535

thermochimica acta

Phase transitions and crystal-field levels in Nd_2NiO_4 ☆

M. Castro, R. Burriel*

Instituto de Ciencia de Materiales de Aragón, CSIC-Universidad de Zaragoza, 50009 Zaragoza, Spain

Received 30 December 1994; accepted 25 May 1995

Abstract

The heat capacity of Nd_2NiO_4 has been measured between 2 and 350 K with adiabatic and ac calorimetry. Thermodynamic functions have been calculated at rounded temperature intervals. The three-dimensional magnetic ordering of the Ni ions produces a small peak in the heat capacity at 325 K, indicating strong two-dimensional magnetic behavior. A sharp first-order peak has been found at 138 K corresponding to the structural transition from the low-temperature tetragonal $P4_2/ncm$ phase to the higher-temperature orthorhombic Bmab phase. No three-dimensional ordering of the Nd sublattice has been detected. The excess heat capacity, after subtracting the estimated lattice contribution, is in agreement with the crystal-field energy levels of the Nd^{3+} ions reported from inelastic neutron diffraction experiments. A broad shoulder below 10 K can be adscribed to an additional splitting of 17 K in the lowest crystal-field doublet of Nd^{3+}. It is due to the interaction with the internal magnetic field created by a canting of the Ni^{2+} magnetic moments.

Keywords: Ac Calorimetry; Adiabatic calorimetry; Crystal-field levels; Heat capacity; Magnetic behavior; Nd_2NiO_4; Phase transition; Thermodynamic functions.

1. Introduction

The R_2NiO_4 compounds (R = rare earth atom) have an orthorhombic structure at room temperature, like La_2CuO_4, with the Ni atoms in octahedral coordination. Their structure can be described as formed by single layers of perovskite-like $LaNiO_3$ shifted (1/2, 1/2, 0) from the adjacent layer and piled up along the *c* axis. The NiO_6 octahedra

* Corresponding author.

☆ Presented at the 6th European Symposium on Thermal Analysis and Calorimetry, Grado, Italy, 11–16 September 1994.

SSDI 0040-6031(95)02544-8

share corners on the *ab* plane forming a two-dimensional network and confining the magnetic exchange interactions inside the Ni–O planes. They present a structural transition, typical of layered perovskites, driven by a slight rotation of the connected NiO_6 octahedra [1].

Independent antiferromagnetic ordering of the Ni and Nd sublattices has been reported at 320 and 11 K, respectively, in Nd_2NiO_4 [2]. Moreover, neutron diffraction and magnetic studies have shown a complex structural and magnetic behavior [1, 2]. Several spin reorientations have been detected in the temperature range between the three-dimensional magnetic ordering temperatures of both sublattices similar to the reported ones for Nd_2CuO_4 [3]. With the transition from the orthorhombic to the low-temperature tetragonal phase, an internal magnetic field develops due to the canting of the Ni^{2+} moments which polarizes and induces a magnetic moment in the Nd^{3+} ions.

Inelastic neutron scattering experiments [4] have determined the crystal-field splitting of the ground multiplet, finding a large intrinsic width of the diffraction peaks. This could be due to oxygen disorder which produces a distribution of crystal fields at the Nd sites, or to the exchange interactions of the Nd^{3+} ions with the Ni sublattice.

Our heat capacity measurement enables checking of the validity of the crystal-field energy levels assigned from the neutron experiment and estimation of the additional effect of the internal magnetic field on the doublet ground state. The existence of three-dimensional ordering of the Ni and Nd sublattices and the type of magnetic interactions are analyzed. The thermodynamic parameters of the transitions are deduced.

2. Experimental

Nonstoichiometric black samples were prepared by solid state reaction, firing stoichiometric amounts of high purity Nd_2O_3 and NiO in air at 1350°C with several intermediate regrindings. The ideal stoichiometry (brown color sample) was obtained by passing a hydrogen flow through the sample for several hours at around 583 K [5].

Adiabatic heat capacity measurements were made in a computerized adiabatic calorimeter operating in the range 5 K–350 K. The amount of sample used was around 3.5 g. The sample was placed in a copper calorimetric vessel of 1 cc provided with an electrical heater and a calibrated platinum-resistance thermometer following the IPTS–90 temperature scale. A few kPa of helium gas inside the vessel enabled thermal equilibrium of the sample to be reached rapidly. Differential thermocouples between the sample vessel and different parts of the adiabatic shields were used to control the adiabaticity with a digital temperature controller interconnected with the measuring program. Data points were usually taken every three degrees, with smaller intervals at low temperatures and near the transitions. The molar heat capacity was obtained by subtracting the contribution of the empty vessel, measured in a separate experiment. The accuracy of the experimental set-up has been established by measuring 5.8 g of copper (OFHC) and comparing the results with the data of Furukawa et al. [6]. At

temperatures lower than 30 K the absolute accuracy is 2%, for $30 < T < 100$ K it is 0.7% and for higher temperatures up to 350 K, 0.3%.

Ac calorimetry has been used in the temperature range where high relaxation times were obtained in the adiabatic measurements. The ac heat capacity experiment has been performed in a commercial ac calorimeter from Sinku-Riko Company (model ACC-1VL). Briefly, the basis of this method is the following: when the sample is heated with a periodic power, its temperature oscillates and can be written as

$$T_s = T_B + \Delta T_{dc} + \Delta T_{ac} \cos(\omega t + \phi) \quad (1)$$

where T_B is the temperature of a copper block, ΔT_{dc} is the average value of the temperature difference between block and sample, ΔT_{ac} the oscillation amplitude, ω the frequency and ϕ the phase shift between the heating power and the temperature oscillations. For a selected frequency, the oscillation amplitude is inversely proportional to the heat capacity. A slab-shaped sample of pressed powder of around 3 mg mass and 0.3 mm thick was used. The selected frequency for the heating power was 1 Hz and the scan rate 30 K h^{-1}, although 10 K h^{-1} has been used at low temperatures. Temperatures below 4.2 K have been obtained by pumping the helium bath with a rotary vacuum pump reaching 2 K. Absolute value were obtained by scaling the relative values to the heat capacity measured by adiabatic calorimetry in the common temperature range.

3. Results and discussion

The heat capacity of Nd_2NiO_4 from 2 to 350 K is shown in Fig. 1. The data below 80 K have been obtained by ac calorimetry scaled to the adiabatic data at this temperature. The measured heat capacity values are listed in Table 1. This table lists only the data obtained by adiabatic calorimetry because ac calorimetry gives only relative values. Table 2 shows the thermodynamic functions calculated at rounded temperature intervals. In order to obtain these functions, the heat capacity has been extrapolated below 2 K assuming the low-temperature-dependence of a Schottky anomaly with two levels.

A small peak at 325 ± 0.5 K corresponds to the long-range ordering of the Ni sublattice. This temperature is in agreement with that reported from magnetic measurement and neutron diffraction experiments [1]. The very small anomalous entropy of the peak, $\Delta S \approx 0.01 R$, implies that most of the magnetic entropy due to the ordering of the Ni^{2+} ions ($\Delta S = R \ln 3$) is consumed in a short-range ordering process over a broad temperature range. The important two-dimensional character of the Ni magnetic interactions is in accordance with the structural feature of linked NiO_6 octahedra on the *ab* plane. The experimental magnetic heat capacity peak at T_N, $\Delta C_{exp}(T_N) \approx 0.2R$, can be compared with the expected theoretical value, which has to be [7]:

$$\Delta C_m(T_N) = \left[\frac{\Delta S_m(T_N)}{\Delta S_m(\infty)}\right] \beta^2 \Delta C_m^{MF}(T_N) \quad (2)$$

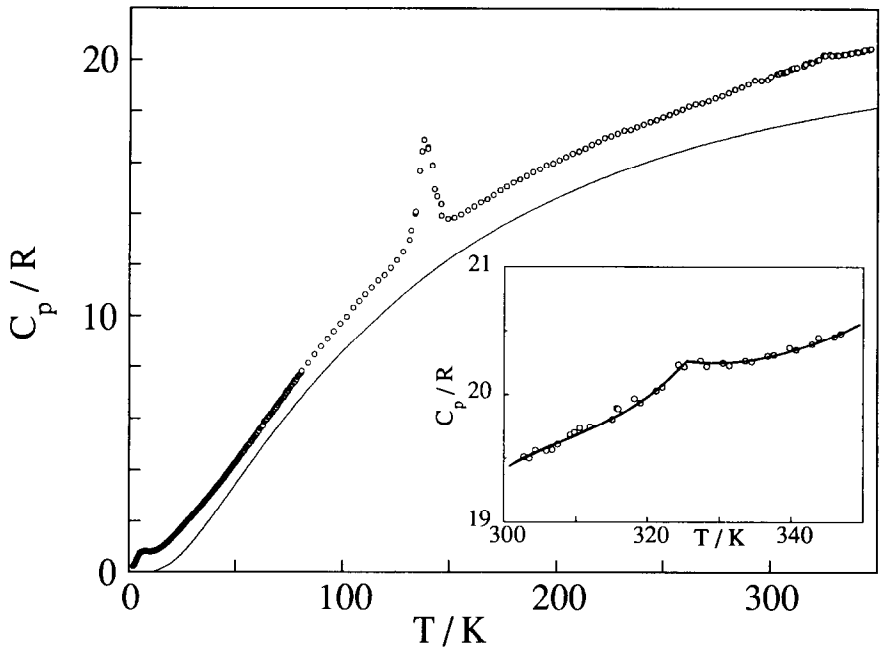

Fig. 1. Heat capacity measurements of Nd_2NiO_4 with adiabatic ($T > 80$ K) and ac ($T < 80$ K) techniques. The lattice contribution, shown as a continuous line, has been calculated from the density of states of La_2NiO_4 given in an inelastic neutron scattering study [15]. The Ni^{2+} magnetic ordering anomaly is shown in the inset as a smooth line through the experimental points.

Table 1
Adiabatic heat capacity data of Nd_2NiO_4

T/K	C_p/R
Series 1	
304.36	19.56
307.42	19.61
310.47	19.73
315.72	19.88
Series 2	
299.82	19.41
302.78	19.51
305.85	19.56
311.93	19.75
315.10	19.81
318.16	19.97
321.25	20.03
324.31	20.23
327.39	20.27

Table 1 (*Continued*)

T/K	C_p/R
330.49	20.25
333.58	20.27
336.68	20.30
339.76	20.37
342.84	20.40
345.92	20.45
Series 3	
309.17	19.69
Series 4	
303.53	19.50
306.66	19.57
309.75	19.70
315.92	19.89
319.00	19.94
322.08	20.06
325.16	20.22
328.24	20.22
331.34	20.23
334.44	20.26
337.54	20.31
340.64	20.35
343.73	20.45
346.83	20.48
Series 5	
80.97	7.856
83.92	8.173
86.87	8.504
89.83	8.819
92.81	9.120
95.77	9.415
98.75	9.709
101.73	9.989
104.71	10.34
Series 6	
107.45	10.60
110.19	10.86
113.19	11.12
116.18	11.40
119.18	11.61
122.18	11.89
125.18	12.19
128.18	12.52
131.17	12.99

Table 1 (*Continued*)

T/K	C_p/R
134.12	14.10
136.97	16.47
139.88	16.58
143.00	14.98
146.19	13.94
149.30	13.81
152.35	13.87
155.40	13.99
158.43	14.15
161.47	14.31
164.50	14.47
167.53	14.60
170.56	14.76
173.59	14.95
176.63	15.09
179.66	15.25
182.70	15.38
185.73	15.51
188.76	15.67
191.80	15.79
194.83	15.94
197.88	16.01
200.91	16.14
203.95	16.26
206.99	16.39
210.04	16.49
213.08	16.59
216.11	16.73
219.16	16.85
222.20	17.00
225.25	17.06
228.29	17.17
231.34	17.29
234.38	17.31
237.43	17.43
240.47	17.53
243.51	17.62
246.55	17.71
249.59	17.81
252.64	17.90
255.68	18.01
258.73	18.11
261.77	18.23
264.82	18.32
267.87	18.35
270.91	18.45
273.95	18.55
277.00	18.65
280.05	18.75

Table 1 (*Continued*)

T/K	C_p/R
283.09	18.88
286.15	18.98
289.20	19.10
292.24	19.24
295.29	19.24
298.34	19.27
Series 7	
131.90	13.36
133.94	14.02
135.89	15.70
137.83	16.91
139.83	16.63
141.91	15.93
144.03	14.70
146.13	14.41

where $\Delta S_m(\infty) = R \ln 3$ is the total magnetic entropy, $\beta = 0.8$ is the spin deviation factor for $S = 1$, $\Delta C_m^{MF}(T_N) = 2R$ is the mean-field value for the magnetic heat capacity jump, and $\Delta S_m(T)$ is the magnetic entropy estimated using spin-wave theory for the antiferromagnetic Heisenberg square lattice [8]. Eq. (2) with a mean value for the exchange intraplanar constant $J = -167$ K obtained from different techniques [9–11] yields $\Delta C_m(T_N) = 0.16R$, in agreement with the experimental data.

A sharp peak at 138 ± 0.5 K due to the structural transition from Bmab to $P4_2/ncm$ phase is shown in Fig. 1. The anomalous entropy $\Delta S = 0.37R$ is two times larger than the corresponding entropy in La_2NiO_4 and Pr_2NiO_4 for the same transition [12]. This difference can be associated with the higher magnetic contribution in this transition coming from the development of a stronger ferromagnetic component along the c-axis. The canting angle of the Ni^{2+} magnetic moments with respect to the basal plane increases on moving from La_2NiO_4 to Nd_2NiO_4 [2]. The sharpness of the peak could indicate a first-order character. To study its character, an ac heat capacity experiment has been performed from 100 to 200 K. The existence of latent heat in a first-order transition produces a sudden change in the phase angle ϕ that enables the character of the phase transition to be established, although the latent heat can not be measured. The results are shown in Fig. 2. The strong linear dependence of the phase angle from 100 to 145 K indicates the presence of a phase coexistence region which finishes at 145 K with a clear change in the phase angle behavior reaching almost a constant value. The maximum heat capacity corresponding to the structural transition appears at 143 K, a higher temperature than the value obtained from the adiabatic measurements, but this shift can be due to the rate of the measurements (30 K h^{-1}) and the absence of equilibrium of phases in this coexistence region. Then, the sudden change in the behavior of the phase angle at 145 K indicates a first-order character for this transition.

Table 2
Calculated thermodynamic functions for Nd_2NiO_4 ($\Phi^\circ_m = \Delta_0^T S^\circ_m - \Delta_0^T H^\circ_m/T$)

T/K	$C^\circ_{p,m}/R$	$\Delta S^\circ_m/R$	$(\Delta H^\circ_m/R)$/K	Φ°_m/R
5	0.735	0.379	1.374	0.104
10	0.831	0.946	5.485	0.397
15	0.986	1.301	9.890	0.641
20	1.348	1.630	15.65	0.847
25	1.806	1.979	23.52	1.038
30	2.274	2.351	33.74	1.226
35	2.756	2.737	46.30	1.414
40	3.248	3.137	61.30	1.604
45	3.765	3.549	78.83	1.797
50	4.319	3.974	99.02	1.994
60	5.431	4.859	147.7	2.397
70	6.576	5.784	207.8	2.814
80	7.735	6.737	279.4	3.245
90	8.841	7.712	362.3	3.687
100	9.827	8.695	455.6	4.138
110	10.85	9.681	559.2	4.597
120	11.72	10.66	672.0	5.062
130	12.83	11.64	793.7	5.530
140	16.69	12.74	942.9	6.004
150	13.82	13.76	1090	6.489
160	14.24	14.66	1230	6.971
170	14.74	15.54	1375	7.450
180	15.26	16.40	1525	7.923
190	15.72	17.23	1680	8.391
200	16.10	18.05	1839	8.854
210	16.50	18.84	2002	9.311
220	16.89	19.62	2169	9.762
230	17.22	20.38	2340	10.21
240	17.51	21.12	2513	10.65
250	17.82	21.84	2690	11.08
260	18.15	22.55	2870	11.51
270	18.44	23.24	3053	11.93
273.15	18.53	23.45	3111	12.06
280	18.74	23.91	3239	12.35
290	19.16	24.58	3428	12.76
298.15	19.27	25.11	3585	13.09
300	19.37	25.23	3621	13.16
310	19.70	25.87	3816	13.56
320	20.02	26.50	4015	13.95
330	20.25	27.12	4216	14.34
340	20.36	27.73	4419	14.73
350	20.54	28.32	4624	15.11

Turning again to Fig. 1, no anomalies have been observed for some reported spin reorientations between 40 and 70 K. Nevertheless, below 100 K, the relaxation time of the equilibrium process after a heat pulse input in the adiabatic experiment increases sharply. This strong increase below 100 K could be associated with some smooth spin reorientations in this temperature range.

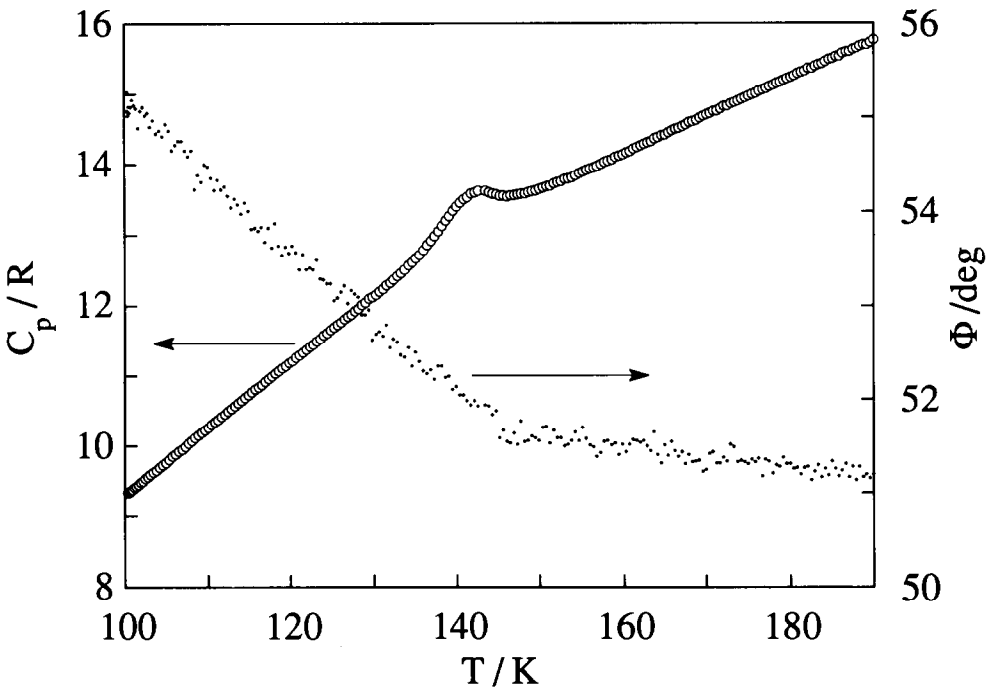

Fig. 2. Structural anomaly obtained in the ac measurements. The heat capacity is represented with circles and the phase given in (1) is shown with dots after shifting the origin by an arbitrary angle.

There is no evidence of the reported three-dimensional ordering of the Nd sublattice but a clear broad shoulder below 10 K can be seen in Fig. 1. This hump is quite similar to the measured anomaly in Nd_2CuO_4 that presents a maximum at 1.7 K [13]. The ac magnetic susceptibility shows two peaks; the first appears at around 11 K and had been related to the long-range order of the Nd^{3+} ions [2]. Such an anomaly can also be due to the splitting of the lowest ground state of Nd^{3+} due to the effective field created by the Ni sublattice, as happens in Er_2BaNiO_5 [14].

In order to obtain an estimate of the electronic energy levels and magnetic contribution of Nd^{3+} at low temperture, one needs to evaluate the lattice heat capacity, C_1. This contribution can be calculated following the Born-von-Kármán model given by

$$C_1 = 3rNk \int_0^\infty \left(\frac{h\nu}{2kT}\right)^2 G(\nu)\, ch^2\left(\frac{h\nu}{2kT}\right) d\nu \tag{3}$$

where $G(\nu)$ is the phonon density of states as a function of frequency and r is the number of atoms per formula unit. The isostructural compound La_2NiO_4, with a nonmagnetic rare earth, has been used for this calculation. The phonon density of states of La_2NiO_4, $G(\nu)$, has been deduced from inelastic neutron scattering measurements and analyzed on the basis of a rigid-ion model [15]. This contribution is shown as a continuous line

in Fig. 1. The excess heat capacity, existing in the whole temperature range for Nd_2NiO_4, after subtracting the phonon contribution, is presented in Fig. 3. Several contributions (anharmonic, magnetic, Schottky, etc.) added together give such an excess.

The Schottky anomaly originates from splitting of the $^4I_{9/2}$ ground multiplet of Nd^{3+} into five doublets when the ion is submitted to a crystal field of tetragonal symmetry. It can be evaluated and compared with our results. Four peaks at energies 93, 267, 441 and 568 K can be resolved from inelastic neutron scattering measurements on Nd_2NiO_4 [4] and represent the complete decomposition of the ground multiplet. The Schottky contribution calculated with this scheme is represented in Fig. 3 for comparison with the experimental data. The excess above 200 K corresponds to the additional contributions coming from the lattice expansion and the Ni magnetic ordering. Qualitative agreement above 50 K can be appreciated but the low-temperature shoulders can not be explained with these levels.

A Zeeman splitting of the Nd^{3+} energy doublets could account for the low-temperature humps of the heat capacity. Moreover, a broadening of the inelastic neutron peaks had been observed [4] suggesting that the exitations could be composed of pairs of peaks. The origin of this splitting of the doublets has to come from the additional interaction of the internal magnetic field produced by the canted Ni^{2+} spins

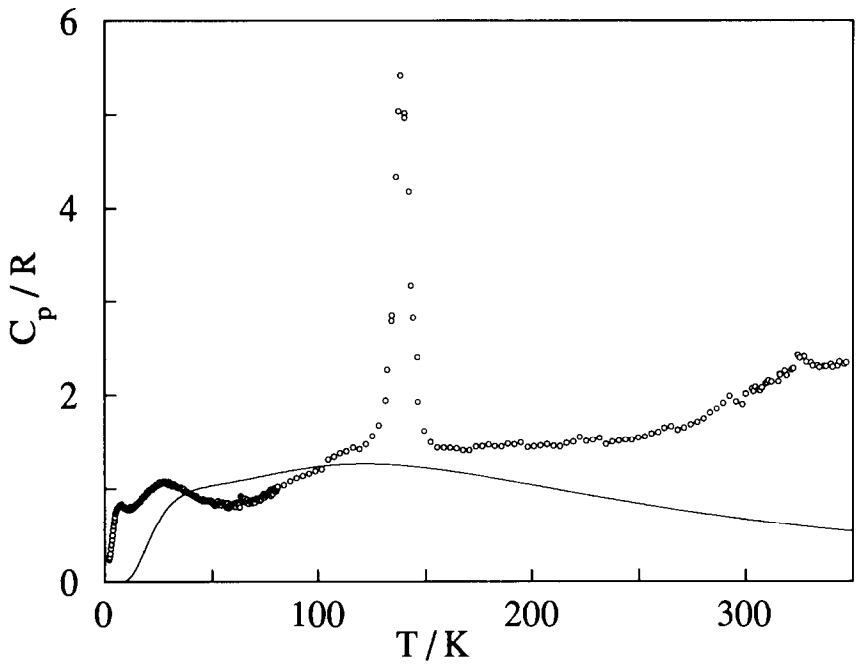

Fig. 3. Anomalous heat capacity of Nd_2NiO_4 after subtraction of the lattice contribution. The continuous line is the Schottky anomaly calculated with the energy splitting of Nd^{3+} given in [4].

on the magnetic moment of Nd^{3+}. This field has been evaluated from magnetic susceptibility measurement to be $H_i = 5.2\,T$ in the 20 to 45 K temperature range, being constant below 20 K [2].

As a first approximation, from the temperature of the first maximum in the excess heat capacity, one can estimate a splitting $\delta = 17\,K$ for the lowest doublet. The theoretical curve can be seen in Fig. 4 for the low-temperature range, where a very good fit to the heat capacity data is obtained. The small differences can be due to a small change with temperature of the splitting of the ground state and the influence of the Nd–Nd exchange interaction, which is active at the lowest temperatures. The corresponding energy splittings of the higher doublets do not much affect the shape of the Schottky anomaly. Only a small displacement of 1 meV, permitted by the uncertainty of the measured energies, has been applied to some levels for a better fit. The inelastic neutron scattering levels and the deduced levels from our calorimetric measurements are shown in Fig. 5.

In order to correlate the susceptibility data with our calorimetric results, one can calculate the parallel susceptibility by following a molecular-field approximation. The first-excited doublet lies at around 100 K, then, below 40 K the ground doublet gives the dominant contribution to the susceptibility. If one considers a small external

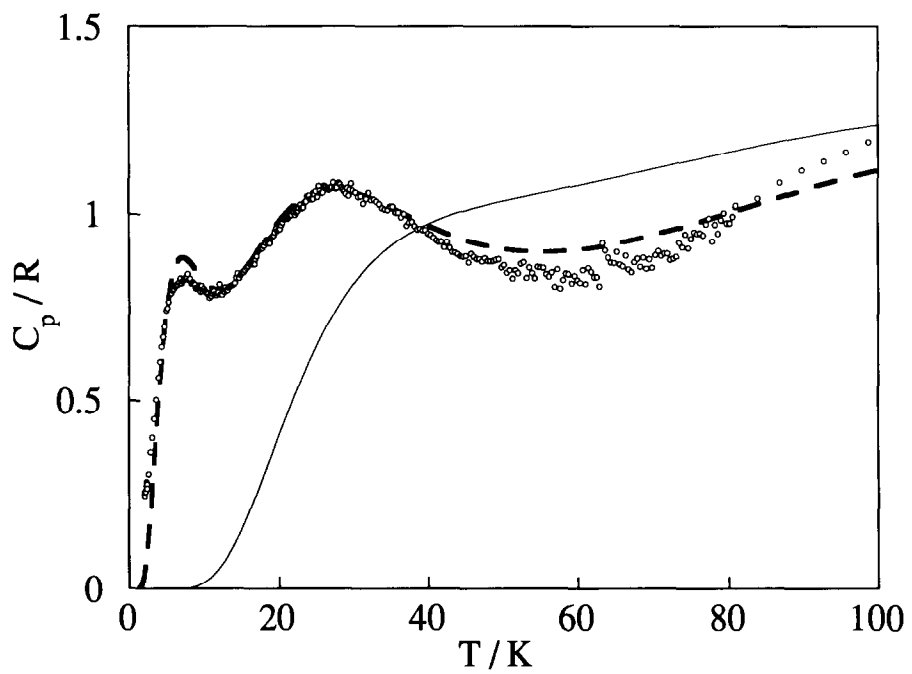

Fig. 4. Low-temperature heat capacity contribution of the Nd^{3+} energy levels. The Schottky contribution of the Nd^{3+} energy levels reported from inelastic neutron scattering [4] is shown as a continuous line. Almost the same levels with additional splitting of 17 K in the ground doublet result in the Schottky anomaly shown with a dashed line.

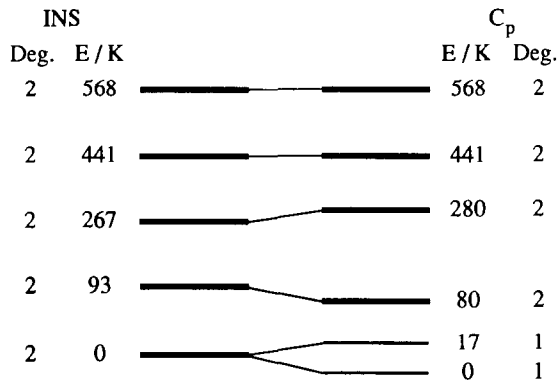

Fig. 5. Schematic diagram of the energy levels and degeneracies of the Nd^{3+} ground multiplet. The left side shows the values from inelastic neutron scattering given in Ref. [4] and the right side the energies that give the best fit to the low-temperature heat capacity data.

magnetic field, the parallel susceptibility is given by

$$\chi_{\parallel} = \left(\frac{2N\mu_B^2 g_{eff}^2}{4kT}\right) sh^2\left(\frac{\delta}{2kT}\right) \tag{4}$$

where $g_{eff} = 4.87$ is estimated from $\delta = g_{eff}\mu_B H_i$. The calculated susceptibility exhibits a maximum at 11 K that coincides with the experimental measurements for a polycrystalline sample [2].

Both, heat capacity and magnetic susceptibility results are explained with a 17 K splitting of the lowest doublet. Moreover, this value is in the range expected from the internal field produced by the ferromagnetic component of the Ni^{2+} magnetic moments. So, one can discount the existence of cooperative magnetic three-dimensional ordering of the Nd^{3+} ions.

Acknowledgements

We thank F. Fernández and R. Saez-Puche, from the Universidad Complutense de Madrid, for providing the samples used in these measurements. This work has been supported by CICYT, Projects PB91-0652 and MAT94-0804.

References

[1] J. Rodríguez-Carvajal, M.T. Fernández-Díaz, J.L. Martínez, F. Fernández and R. Saez-Puche, Europhys. Lett., 11 (1990) 261.
[2] X. Batlle, X. Obradors and B. Martínez, Phys. Rev. B, 45 (1992) 2830.
[3] M. Matsuda, K. Yamada, K. Kakurai, K. Kadowaki, T.R. Thurston, Y. Endoh, Y. Hidaka, R.J. Birgeneau, M.A. Kastner, P.M. Gehring, A.H. Moudden and G. Shirane, Phys. Rev. B, 42 (1990) 10098.

[4] A.T. Boothroyd, S.M. Doyle, M.P. Sridhar, D. McK. Paul and R. Osborn, J. Less-Common Met., 164–165 (1990) 915.
[5] R. Saez-Puche, F. Fernández, J. Rodríguez-Carvajal and J.L. Martínez, Solid State Commun., 72 (1989) 273.
[6] G.T. Furukawa, W.G. Saba and M.L. Reilly, NSRDS-NBS18 (1968).
[7] K. Sun, J.H. Cho, F.C. Chou, W.C. Lee, L.L. Miller, D.C. Johnston, Y. Hidaka and T. Murakami, Phys. Rev. B, 43 (1991) 239.
[8] R. Kubo, Phys. Rev., 87 (1952) 568.
[9] X. Batlle, X. Obradors, M.J. Sayagués, M. Vallet and J. González-Calbet, J. Phys.: Condens. Matter, 4 (1992) 487.
[10] K. Nakajima, K. Yamada, S. Hosoya, T. Omata and Y. Endoh, J. Phys. Soc. Jpn., 62 (1993) 4438.
[11] Th. Strangfeld, K. Westerholt and H. Bach, Physica C, 183 (1991) 1.
[12] M. Castro and R. Burriel, Heat capacity study of La_2NiO_4 and Pr_2NiO_4, Thermochim. Acta, (this issue).
[13] S. Ghamaty, B.W. Lee, J.T. Markert, E.A. Early, T. Bjørnholm, C.L. Seaman and M.B. Maple, Physica C (1989) 217.
[14] G.G. Chepurko, Z.A. Kazei, D.A. Kudrjavtsev, R.Z. Levitin, B.V. Mill, M.N. Popova and V.V. Snegirev, Phys. Lett. A, 157 (1991) 81.
[15] L. Pintschovius, J.M. Bassat, P. Odier, F. Gervais, G. Chevrier, W. Reichardt and F. Gompf, Phys. Rev. B, 40 (1989) 2229.